Time-dependent distortion in calculations of K-shell ionization for incident protons and helium and lithium ions

David J. Land
Naval Surface Warfare Center, Silver Spring, Maryland 20903-5000
(Received 2 May 1990; revised manuscript received 13 March 1991)

Time-dependent distortion of the initial electronic state in response to the motion of the projectile is employed in calculations of total and differential cross sections for the direct-Coulomb, K-shell-ionization process within the semiclassical approximation. Selected targets are chosen from Al through Ag for incident protons and helium and lithium ions in the velocity region that corresponds to energies of 0.175 through 5.0 MeV/u for a Cu target. The distortion is taken to include both energy and wave function (via polarization) of the initial-state K-shell electron. Discussion is presented with regard to the appearance of nonorthogonal basis states. The results of calculations for the total K-shell-ionization cross section in comparison with experimental data show good agreement for protons incident on targets from Ti through Cu. Some differences are noted for Al and Ag targets, and systematically larger discrepancies with projectile atomic number are obtained for He and Li projectiles. It is found that the introduction of temporally dependent distortion causes drastic changes in the behavior of the scattering amplitude at low velocities that have not been generally appreciated. Time-dependent binding gives rise to a large suppression of the cross section (over that induced by the well-known introduction of a constant increase in binding), while time-dependent polarization leads to a large enhancement. An explanation of this behavior is suggested. Possible causes of the differences between theoretical and experimental values of the cross section are considered. Some observations apropos of the introduction of temporally dependent quantities in approximate calculations are made.

I. INTRODUCTION

Considerable progress is being achieved in calculations of ion-atom collisions in general and of ion-induced ionization in particular. Recent examples of special note include the single ionization of hydrogen and helium by protons and antiprotons for both total and differential cross sections [1] and the double ionization of He by protons and antiprotons [2]. Good correlation is found between theoretical calculations and experimental data [3]. It might be expected, therefore, that close agreement would be found for the seemingly more straightforward problem of the direct-Coulomb ionization, induced by light ions, of the innermost shell of an atom for asymmetric collision systems satisfying $Z_P \leq 0.3 Z_T$, where Z_P and Z_T are the atomic numbers of the projectile ion and target atom, respectively. Calculations [4,5] of the total cross section, which include many features of the physics of inner-shell ionization, show close agreement with experimental data for incident protons. However, results from second-order Born and sophisticated, coupled-channel numerical calculations [6] for incident protons differ from experiment by 10% for heavier targets (nickel) to as much as 25% for lighter targets (carbon) with the theoretical values systematically low [7]. There is indication that similar calculations [8] for incident helium ions show a larger discrepancy [7]. Other calculations [5] for incident He and Li ions reveal an increasingly larger systematic deviation from experiment as Z_P is increased. Thus the relatively close agreement observed in some instances for the proton data may be somewhat fortuitous.

The present paper is part of a combined experimental-theoretical effort at the Naval Surface Warfare Center (NSWC) in the investigation of inner-shell ionization. Experimental measurements have been performed at NSWC for the proton- and ^{3}He and ^{4}He ion-induced total K-shell ionization cross sections and have been reported previously [9]. Measurements have also been made at NSWC for the cross-section differential in the projectile scattering angle and are reported in a separate publication [10]. This paper develops a coherent account of a theoretical description of the inner-shell ionization process for asymmetric systems in which several physical phenomena that are believed to govern the process are taken into account. The velocity region of interest in these studies lies within the region $0.2 \lesssim \xi \lesssim 1.2$, where ξ is the ratio of the adiabatic radius, $\hbar v / E_B$, to the K-shell radius, $1/(Z_T - 0.3)$, v is the projectile velocity, and E_B is the binding energy of the K-shell electron. This region thus corresponds to projectile velocities less than or equal to the electron orbital velocity.

Inner-shell ionization induced by a heavy ion is often described theoretically within the impact parameter formulation or, equivalently, the semiclassical approximation (SCA), following the pioneering work of Bang and Hansteen [11,12]. The conditions for this approximation are often well satisfied for a heavy projectile and the mathematical expressions for the scattering amplitude are less complicated in terms of both analysis and numerical evaluation than those for the corresponding fully quantal treatment. Within this approach it is convenient to study in a systematic way two physical phenomena

that are considered to play a major role in the inner-shell ionization process. These have been labeled as the binding effect and the polarization effect. Within the single-particle approximation, the active electron responds to the time-varying field of the intruding projectile through a distortion of its energy in terms of an increase (or decrease) in its binding energy for a positively (or negatively) charged projectile [13,14] and a distortion or polarization of its wave function [15,16]. Past calculations [4,5] of inner-shell ionization for low-velocity projectiles have often been performed with the approximation that both the binding energy and wave function be evaluated for the projectile fixed at or near the position of the target nucleus, under the rationale that ionization occurs most probably when the projectile is close to the target nucleus. If, however, we choose to work within the SCA, then it is of interest to see what are the effects of temporally dependent binding energy and wave functions for the electron. This paper considers this issue and reports the results of calculations of the total cross section for K-shell ionization in which such time dependence is incorporated.

The time dependence of the initial-state electron binding energy has been considered previously in several calculations [17–19] of inner-shell ionization. A sharp decrease in the total cross section at low energies in comparison with the results of the first Born approximation or other forms of perturbation theory was found. Calculations by the present author [20], in which a Coulomb trajectory [21] was used to describe the motion of the projectile and other well-known effects were estimated, showed that the incorporation of an apparently improved treatment of electron binding resulted in poor agreement in comparison with experimental data for asymmetric collisions at low projectile velocities.

While the incorporation of energy distortion in a time-independent or time-dependent way is straightforward, treatments of wave-function distortion have been varied. Within the SCA a traditional model [4,22] employs an initial-state wave function evaluated in the united-atom limit; i.e., a K-shell wave function for a target nucleus having an atomic number equal to the target plus projectile is used. Alternatively, an elaboration [16,23] of this model assumes a K-shell wave function evaluated with an effective charge that is determined from a minimization of the total energy [Eq. (4) below] corresponding to the distance of closest approach. Both models thus incorporate only a monopole distortion of the wave function. In an approach designed to introduce a dipole distortion of the electron wave function, Basbas, Brandt, and Laubert [15] employed the simple harmonic-oscillator model for the electron shell. This modification was one of several corrections to the plane-wave Born approximation for inner-shell ionization. More recently, Basbas and Land [24] constructed an initial-state, multipole wave function that exhibits polarization induced by the projectile and consists of an undistorted wave function multiplied by a factor that allows charge to build about the projectile.

As noted previously, the overall goal of the present investigation is to incorporate the full temporal dependence of both the electron binding and wave function in K-shell ionization. Hence, the multipole wave function of Ref. [24] was subsequently employed in (unpublished) calculations of the ionization probability that included this time dependence. A significant enhancement in the ionization probabilities was found and this appeared to cancel, at least in part, the suppression induced by binding alone. This result was quite surprising and, in order to study its origins, an electronic wave function, which consists explicitly of a spherically symmetric contracting term (monopole) and a dipole term, was advanced [25] as an alternative to the multipole wave function, which was difficult to deconvolute. The enhancement in the ionization probabilities was found to arise explicitly from the temporal variation of the monopole component of the wave function and not from the dipole part. A qualitative discussion of both the suppression from binding and enhancement from polarization is given below.

In the present paper, this model, involving the monopole and dipole wave function, is applied in calculations of the K-shell-ionization cross section from low through moderate velocities for incident protons and helium and lithium ions. The systems studied include a wide range of target atoms from Al through Ag for which experimental data are available. The theoretical results are shown in comparison with experimental data. Good agreement is obtained for incident protons in comparison with the NSWC data [9]. However, a systematic and increasingly larger discrepancy is observed for incident He ions and Li ions as the projectile atomic number increases. A broader comparison of the theoretical results with the reference cross sections of Paul and Muir [26] for incident protons shows a larger discrepancy for Al and Ag targets.

It is noted that similar calculations, which employ the multipole wave function of Basbas and Land [24] and in which the time dependence of both binding energy and polarization are considered, were recently reported by Trautmann and Kauer [27]. While the results of the calculations in comparison with experimental data are similar to the present calculations, the authors of this paper conclude a somewhat more favorable overview of the theory than what will be reached here.

Throughout this work atomic units are generally used ($m_e=e=\hbar=1$); in addition, the notation (u, Av) is used to represent the matrix element $\int d\mathbf{r}\, u^*(\mathbf{r}) Av(\mathbf{r})$, where u and v are basis states and A is a quantum-mechanical operator in the coordinate-space representation.

II. THEORETICAL CONSIDERATIONS

A. Hamiltonian

The Hamiltonian H is written as the sum of an atomic part H_a and an interaction $V(t)$:

$$H=H_a+V(t)\ , \tag{1a}$$

where

$$H_a=-\tfrac{1}{2}\nabla^2-\frac{Z_{TK}}{r}-V_s\ , \tag{1b}$$

$$V(t)=-\frac{Z_P}{|\mathbf{r}-\mathbf{R}(t)|}-\frac{Z_P Z_T}{M_T}\frac{\mathbf{R}\cdot\mathbf{r}}{R^3}+W(R)\ , \tag{1c}$$

and where M_T is the mass of the target nucleus, and $\mathbf{r}$ and $\mathbf{R}(t)$ are the coordinates of the electron and the classically prescribed trajectory of the projectile.

The form of H_a presupposes hydrogenic basis states, denoted by ϕ_n, at least asymptotically. The use of $Z_{TK}=Z_T-0.3$ invokes the Slater prescription for the inner screening of the active K-shell electron by the second electron, and the appearance of V_s, a constant shift in energy, implies the Merzbacher-Lewis [28] prescription to account for screening by the outer electrons. V_s is given by $V_s=-\frac{1}{2}Z_{TK}^2+|E_B|$, where E_B is the experimentally determined value of the binding energy of the K-shell electron.

The interaction $V(t)$ is given by the sum of three terms $V_{\text{Coul}}+V_{\text{recl}}+W(R)$. The first term V_{Coul} represents the Coulomb potential between the incoming projectile and the target electron. The second term V_{recl} describes the effect on the system of the recoil of the target nucleus under the influence of the projectile, and has been discussed elsewhere [29]. The third term $W(R)$, which may include the projectile-nucleus potential, is an arbitrary function of $R(t)$. An exact solution of the Schrödinger equation is independent of $W(R)$ (gauge invariance). It is desirable that approximate solutions, such as the present one, maintain this property.

B. Initial-state wave function

The basic motivation behind the present model is to employ within a perturbative approach basis states that describe approximately the behavior of the system in interaction with the perturbing projectile. This approach contrasts with the more usual one of expanding the scattering amplitude in terms of the eigenstates ϕ_n of H_a above. The goal is to minimize coupling among the excited states of the system, or, equivalently, to diagonalize a larger part of the total Hamiltonian within the given basis states.

An initial-state wave function $\Psi_{\text{pol}}(\mathbf{r},\mathbf{R}(t))$, which describes the polarization induced by the passing projectile, is expressed as [25]

$$\Psi_{\text{pol}}(\mathbf{r},\mathbf{R}(t))=R_{\text{pol}}(\mathbf{r},\zeta)Y_{00}(\hat{\mathbf{r}})\ , \tag{2}$$

where

$$R_{\text{pol}}(\mathbf{r},\zeta)=N(R)[1+\lambda(R)r\cos\theta']R_B(r,\zeta(R))\ ,$$

$$R_B(r,\zeta(R))=2\zeta(R)^{3/2}e^{-\zeta(R)r}\ ,$$

and $N(R)=[1+(\lambda/\zeta)^2]^{-1/2}$ is a factor to guarantee unit normalization. θ' is the angle between the projectile coordinate $\mathbf{R}(t)$ and the electron coordinate $\mathbf{r}$ in a coordinate system whose origin is centered on the target nucleus. This wave function is thus seen to consist of a monopole term and a dipole term that depend upon $R(t)$, both multiplied by a spherically symmetric K-shell radial wave function that also depends upon $R(t)$. The angular term involving $\cos\theta'$ can be expressed in terms of the laboratory coordinate system by the addition theorem for spherical harmonics,

$$\cos[<\hat{\mathbf{R}},\hat{\mathbf{r}})]=\frac{4\pi}{3}\sum_{m''}Y^*_{1m''}(\hat{\mathbf{R}})Y_{1m''}(\hat{\mathbf{r}})\ .$$

The functions $\zeta(R)$ and $\lambda(R)$ are determined separately by means of variational principles. The quantity $\zeta(R)$, which plays the role of an effective charge, is obtained with $\lambda(R)$ set to zero by the variational principle of Ref. [22] in which the total energy,

$$\begin{aligned}E_i(t)&=(\Psi_{\text{pol}},H(t)\Psi_{\text{pol}})\\&=-\tfrac{1}{2}Z_{TK}^2+V_s+\tfrac{1}{2}(\zeta-Z_{TK})^2\\&\quad-\frac{Z_P}{R}[1-(1+\zeta R)e^{-2\zeta R}]\ ,\end{aligned} \tag{3}$$

is minimized with respect to $\zeta(R)$. This yields for $\zeta(R)$

$$\zeta(R)=Z_{TK}+Z_P(1+2\zeta R)e^{-2\zeta R}\ . \tag{4}$$

The function $\lambda(R)$ is determined by a subsequent minimization of the energy (without recoil) with respect to $\lambda(R)$ with $\zeta(R)$ held fixed. Details are relegated to Appendix A. For asymmetric systems $\lambda(R)$ is given to a very good approximation by

$$\begin{aligned}\lambda(R)&=2\frac{Z_P}{(\zeta R)^2}[1-e^{-2\zeta R}(1+2\zeta R+2\zeta^2R^2+\zeta^3R^3)]\\&\quad+O(Z_P/Z_{TK})^2\ .\end{aligned} \tag{5}$$

For small R, $\lambda(R)$ has the limiting behavior

$$\lambda(R)\approx\tfrac{2}{3}Z_p\zeta R\ .$$

The function $\lambda(R)$ is related to the dipole moment $\mathbf{D}=(\Psi_{\text{pol}},\mathbf{r}\Psi_{\text{pol}})=|\mathbf{D}|\hat{\mathbf{R}}$ by

$$2\frac{\lambda}{\zeta}=|\mathbf{D}|\zeta\left[1+\left[\frac{\lambda}{\zeta}\right]^2\right]\ .$$

(Components of $\mathbf{D}$ perpendicular to $\hat{\mathbf{R}}$ are zero by the symmetry of the wave function.) For asymmetric systems the term $(\lambda/\zeta)^2$ is negligible.

The polarized wave function $\Psi_{\text{pol}}(\mathbf{r},\mathbf{R}(t))$ so determined thus has the following properties: (i) as $R\to\infty$, Ψ_{pol} is an exact eigenfunction of the Hamiltonian Eq. (1) in the separated-atom limit, since $\zeta(R)\to Z_{TK}$ and $\lambda(R)\to 0$; (ii) as $R\to 0$, Ψ_{pol} is an exact eigenfunction of H (without recoil) in the united-atom limit, since $\zeta(R)\to(Z_{TK}+Z_P)$ and $\lambda(R)\to 0$; (iii) as $Z_P\to 0$, the unperturbed state is recovered.

In a previous investigation, Basbas and Land [24] introduced a different wave function that also incorporates projectile-induced polarization:

$$\begin{aligned}\Psi_{\text{pol}}(\mathbf{r};\mathbf{R})&=N(R)[e^{-Z_P|\mathbf{r}-\mathbf{R}|}+f(R)]\\&\quad\times 2Z_{TK}^{3/2}e^{-Z_{TK}r}/\sqrt{4\pi}\ .\end{aligned} \tag{6}$$

As before, $N(R)$ is determined to give unit normalization to the wave function; $f(R)$ is again determined by a vari-

ational principle in which the total energy is minimized. In this wave function the electron cloud builds about the projectile in a K-shell-like fashion as the projectile nears the target nucleus. Unlike the initial-state wave function of Eq. (2), which consists of monopole and dipole moments only, this wave function is comprised of all moments. However, it is not clear how to resolve the various multipole contributions to the total amplitude, a circumstance which proves desirable.

Similar forms of a wave function containing polarization have been considered previously. Temkin [30] employed a polarized orbital in a wave treatment of electron-hydrogen scattering. Kleber and Unterseer [31] introduced a wave function quite similar in form to that of Eq. (2) in calculations of K-shell ionization. Their approach develops a wave function from a dynamical, variational principle as a solution of the complete time-dependent Schrödinger equation. The S matrix is obtained on the basis of closure. Unfortunately, the application of this solution was limited to the systems p in Cu and d in Cu, processes which seem not to stress the theory.

It should be noted that the description of the electron cloud through a spherically symmetric (monopole) contraction and expansion of the wave function has been discussed by other authors. Laegsgaard, Andersen, and Lund [22] have considered its influence on the screening factor V_s contained in H_a above. Benka, Geretschläger, and Paul [32] introduced this effect as a further correction to the energy-loss Coulomb-deflection perturbed-stationary-state relativistic (ECPSSR) model of Basbas, Brandt, and Laubert [14] and Brandt and Lapicki [33]. This group notes that this description for low projectile velocities amounts to the use of the correct K-shell electron velocity in the united-atom limit, to be distinguished from the use of the correct electron binding energy [13] in this limit, which is included in the ECPSSR model.

C. Final-state wave function

The wave functions describing the final states of the electron which, for the problem of ionization, are continuum states are chosen as the eigenfunctions ϕ_n of the atomic Hamiltonian H_a. In principle, the final states could also exhibit a distortion or polarization induced by the projectile, and the continuum-distorted-wave eikonal-initial-state model of Crothers and McCann [34] utilizes such states. An immediate interest of those authors was to study the effect of the projectile on emitted electrons that are close to the projectile. These studies were subsequently extended by Fainstein, Ponce, and Rivarola [1] specifically for incident antiprotons. Such states would be required for studies, performed within the context of perturbation theory, involving capture to the continuum of the projectile. Because the states of the projectile continuum contribute very little to total or differential (in the projectile scattering angle) cross section, simple unperturbed eigenfunctions of H_a are used.

The radial part of these eigenstates for angular momentum l is written [35]

$$R_{kl}(r)=\frac{C_{Ek}}{(2l+1)!}(2kr)^l e^{-ikr} \times F(i/k+l+1,2l+2,2ikr) , \quad (7)$$

where the normalization constant C_{Ek} is given on the energy scale by

$$C_{Ek}=\frac{2}{(1-e^{-2\pi/k})^{1/2}}\prod_{s=1}^{l}\left[s^2+\frac{1}{k^2}\right]^{1/2} ,$$

and $F(i/k+l+1,2l+2,2ikr)$ is confluent hypergeometric function. In these expressions the variable k does not represent the momentum of the outgoing electron because of the presence of the screening potential V_s in the Hamiltonian. Rather, it is a parameter related to the final-state electron energy E_f by

$$k=[2(E_f+V_s)]^{1/2} ;$$

for $E_f<|V_s|$, k is purely imaginary, and the radial wave function $R_{kl}(r)$ becomes infinite exponentially as $r\to\infty$. This circumstance is well known [28] in this application and causes no problem when this wave function is used in matrix elements involving states bound sufficiently strongly.

In the calculations reported here, the continuum radial wave functions R_{kl} were readily obtained through a numerical solution of the Schrödinger equation by the Runge-Kutta method. This was extended out to 36 times the K-shell radius.

D. Scattering amplitude

In writing an expression for the scattering amplitude, it must be borne in mind that the present model is developed in terms of basis states that are more general than the usually employed unperturbed eigenfunctions of the atomic Hamiltonian H_a. The initial-state wave function $u_i(t)=\Psi_{\rm pol}$ may be regarded as a member of a set of basis states $\{u_n(t)\}$, of which the remaining members are obtained from the excited bound and continuum states of the system. Collectively these functions in general form a set of nonorthogonal states that are not rigorously complete. Nevertheless, they can be used as an acceptable basis provided that the lack of orthogonality is taken into account and that symmetry properties of the Schrödinger equation, such as gauge invariance, are maintained.

Consider a set of basis states $\{u_n(\mathbf{R}(t))\}$. Assume that all states of the set, except for the ground state, which represents the initial state of the system, are mutually orthogonal, although, for the moment, possibly dependent on $\mathbf{R}(t)$. They are chosen to satisfy the boundary conditions

$$\lim_{t\to\pm\infty} u_n(t)=\phi_n ,$$

where the ϕ_n are the time-independent eigenfunctions of the atomic Hamiltonian H_a. By the usual procedure, the expansion of the solution $\psi(t)$ of the Schrödinger equation in terms of these states,

$$\psi(t)=\sum_n a_n(t)u_n(t) ,$$

is substituted into the Schrödinger equation to yield a set of coupled equations for the amplitudes $a_m(t)$:

$$i\frac{d}{dt}a_m=\sum_n a_n(u_m,Hu_n)-i\sum_{n\neq m} a_m\left[u_m,\frac{\partial}{\partial t}u_n\right] -i\frac{d}{dt}a_i(u_m,u_i) .$$

The unitary transformation

$$a_n(t)=\exp\left[-i\int dt'H_{nn}(t')\right]b_n(t) \tag{8}$$

removes the diagonal terms from the right-hand side of these equations. The introduction of perturbation theory at this point (often called the distortion approximation [17,19]), whereby it is assumed $b_n \ll b_i \approx 1$ and $db_i/dt \approx 0$, yields for the amplitude $b_f(\infty)$ of a final state f the expression

$$b_f(\infty)=-i\int_{-\infty}^{\infty} dt \exp\left[i\int_0^t dt'[H_{ff}(t')-H_{ii}(t')]\right]\left[\left[u_f,\left[H-i\frac{\partial}{\partial t}\right]u_i\right]-H_{ii}(u_f,u_i)\right] . \tag{9}$$

This amplitude is manifestly gauge invariant; i.e., it is independent of $W(R)$. However, as the amplitude is expressed in terms of the nonorthogonal basis set $\{u_n\}$, the presence of the overlap integral involving the initial and final states is crucial for this property to hold. It should be noted that the use of perturbation theory does not imply an expansion in Z_P/Z_T, as each term in general contains contributions to all orders in Z_P/Z_T, but rather an expansion in the amplitudes b_n.

In the present model only the initial state of the system is chosen time dependent and the final states are taken as the time-independent, unperturbed eigenstates of H_a, ϕ_n. Further development of Eq. (9) is specialized to this case. One first notes that

$$\left[u_f,\frac{\partial u_i}{\partial t}\right]=\frac{\partial}{\partial t}(u_f,u_i) ,$$

because the $u_f=\phi_f$ are here independent of time, and then performs an integration by parts to accomplish effectively the indicated time differentiation of u_i. The expression for $b_f(\infty)$ becomes

$$b_f(\infty)=-i\int_{-\infty}^{\infty} dt \exp\left[i\int_0^t dt'(H_{ff}-H_{ii})\right] \times[(u_f,Vu_i)-V_{ff}(u_f,u_i)] . \tag{10}$$

This expression resembles the result of lowest-order perturbation theory for the final-state amplitude in the SCA with the addition of the term involving the overlap of the nonorthogonal initial and final states. The appearance of the interaction potential V in Eq. (10) results from the choice that the final states of the system u_f are exact eigenfunction of the atomic Hamiltonian H_a. It has been shown previously [20] that when f refers to a continuum state, the diagonal matrix element V_{ff} can be considered as small as one wishes for numerical purposes, so that the term plays no role in the numerical evaluation of the amplitude, and can be dropped. Nevertheless, its role in preserving the gauge invariance of the theory is again stressed. For problems involving excitation to a bound state, this term is nonvanishing. It is also nonvanishing in formulations that employ pseudostates to represent the continuum states of the system.

It is worth noting that the expression for $b_f(\infty)$, Eq. (10), can also be obtained from other methods in atomic scattering theory and that there is agreement among the results through terms of the order of $(Z_P/Z_T)^2$. One of these is the standard two-state approximation [36,37]. In this approach, a trial solution $\psi_T(t)$ of the Schrödinger equation is written as the sum of two states ψ_i and ψ_f with arbitrary coefficients:

$$\psi_T(t)=c_i(t)\psi_i(t)e^{-iE_it}+c_f(t)\psi_f e^{-iE_ft} .$$

The coefficients c_i and c_f are determined variationally, e.g., with the variational principle of Sil [36,38]. In the present case the functions ψ_i and ψ_f are chosen to be Ψ_{pol} and ϕ_f, respectively. In the general case, care must be given to insure that the two states ψ_i and ψ_f satisfy the proper boundary conditions at $t=\pm\infty$. Equation (10) follows through terms of the order of $(Z_P/Z_T)^2$, if it is assumed that $c_f \ll c_i$.

An alternative point of view can be found in the method of symmetric orthogonalization developed by Crothers [39]. Here one constructs to some order in a small parameter a set of complete, orthogonal states. In the present problem the small parameter is, clearly, Z_P/Z_T, although in other cases another parameter, such as velocity, could be appropriate. This procedure also implies the applicability of Eq. (10) for the scattering amplitude $b_f(\infty)$ and is again in agreement through order $(Z_P/Z_T)^2$.

In summary, the model for ionization to a continuum state is implemented with the following expression for the

scattering amplitude $b_f(\infty)$:

$$b_f(\infty)=-i\int_{-\infty}^{\infty}dt\,\exp\left[i\int_0^t dt'[E_f-E_i(t')]\right]\times(\phi_f,V(t)\Psi_{\rm pol}(\mathbf{R}(t)))\ . \tag{11}$$

This expression, which is effectively gauge invariant in the context of ionization (but not excitation), is not to be regarded simply as a generalized form of the usual expression of the scattering amplitude obtained within the SCA from lowest-order perturbation theory, with a time-dependent initial-state energy and wave function replacing the more normal time-independent, unperturbed forms. Rather, it is obtained by expanding the solution of the Schrödinger equation in a suitable set of basis states that includes the state $\Psi_{\rm pol}(\mathbf{R}(t))$ describing the K-shell electron.

The final state f consists of an electron of energy E_f and angular momentum lm. Thus, within the SCA $|b_f(\infty)|^2$ represents the differential probability for the ejection from the K shell of an electron with energy E_f and angular momentum lm for a projectile with a definite impact parameter b. The probability for ionization at this impact parameter $P(b)$ is obtained by summing over all energies and angular momentum states. The total K-shell-ionization cross section σ is obtained by summing $P(b)$ over all impact parameters $\sigma=2\int 2\pi b\,db\,P(b)$, in which an additional factor of 2 is included to account for the two electrons in the K shell.

E. Matrix elements of the potential

The matrix element of the interaction potential $V(t)$ appearing in Eq. (11) for the scattering amplitude involves the initial, distorted state of Eq. (2) and the final continuum Coulomb state of Eq. (7), having energy E_f and angular momentum lm. This matrix element may be written

$$V^{k,lm}(\mathbf{R})=(\phi_f,V(t)\Psi_{\rm pol}(\mathbf{R}(t)))=\int d\mathbf{r}R_{kl}(r)Y_{lm}^*(\hat{\mathbf{r}})V(\mathbf{r},\mathbf{R}(t))\times R_{\rm pol}(\mathbf{r},\zeta)Y_{00}(\hat{\mathbf{r}})\ ,$$

where V is given in Eq. (1) above. The two parts of V, $V_{\rm Coul}$ and $V_{\rm recl}$, are considered separately. The evaluation of each part can be found straightforwardly with the help of some well-known formulas [40] following from angular momentum theory and noted for reference in Appendix B. The piece involving the Coulomb interaction between the projectile and the electron is based upon the expansion

$$\frac{1}{|\mathbf{r}-\mathbf{R}|}=\sum_{l,m}\frac{4\pi}{2l+1}\frac{r_<^l}{r_>^{l+1}}Y_{lm}^*(\hat{\mathbf{R}})Y_{lm}(\hat{\mathbf{r}})\ , \tag{12}$$

in which the frequently employed notation $r_<$ ($r_>$) is used for the lesser (greater) of r and R. One finds

$$V_{\rm Coul}^{k,lm}(R)=-Z_P\frac{\sqrt{4\pi}}{2l+1}Y_{lm}^*(\hat{\mathbf{R}})N(R)\times\left\{\int_0^\infty dr P_{kl}(r)P_B(r,\xi)\frac{r_<^l}{r_>^{l+1}}\times\left[1+\lambda r\left[\frac{l}{2l-1}\frac{r_<^{-1}}{r_>^{-1}}+\frac{l+1}{2l+3}\frac{r_<}{r_>}\right]\right]\right\}. \tag{13}$$

For the contribution from target recoil one has

$$V_{\rm recl}^{k,lm}(R)=-Z_P\frac{\sqrt{4\pi}}{2l+1}Y_{lm}^*(\hat{\mathbf{R}})N(R)\frac{Z_T}{M_T}\frac{F_l(\lambda/3)}{R^2}\times\int_0^\infty dr\,r^{1+|l-1|}P_{kl}(r)P_B(r,\xi)\ , \tag{14}$$

where $F_l(\lambda/3)$ has the forms $\lambda/3$, 1, and $2\lambda/3$ for the cases $l=0$, 1, and 2, respectively, and is zero for $l>2$. In these expressions the notation $P_{kl}\equiv rR_{kl}$, $P_B\equiv rR_B$ has been introduced. The calculations reported below include s-, p-, and d-wave final states.

F. Numerical methods

The matrix elements of the potential developed above are used in Eq. (11) in the evaluation of the scattering amplitude. Equation (11) is basically the Fourier transform of $V^{k,lm}(\mathbf{R}(t))$ with respect to $\exp(i\omega t)$, where $\omega=E_f-E_i(\infty)$, in which additional oscillatory factors to be discussed below also occur. A scrutiny of $V^{k,lm}(\mathbf{R}(t))$ shows that it can be written as a sum of terms having one of two different asymptotic behaviors: $\exp(-Z_{TK}R)$ or $1/R^n$, with $n\geq 2$. In order to insure good numerical accuracy in the evaluation of this Fourier integral, emphasis was placed on developing numerical methods that reproduce known results for integrands having similar asymptotic behaviors. For simplicity in this discussion, the unit of length is taken as the K-shell radius $1/Z_{TK}$.

For terms having the asymptotic behavior $\exp(-R)$, the following Fourier transform serves as a suitable model [41]:

$$\int_{-\infty}^{\infty}dz\,e^{iwz}e^{-(z^2+b^2)^{1/2}}=\frac{2b}{(w^2+1)^{1/2}}K_1(b(w^2+1)^{1/2})\ , \tag{15}$$

where $w=\omega/v=\xi^{-1}$ and K_1 is a modified Bessel function. It is found that an upper limit of $z=24$ (times the K-shell radius) is sufficient for integrals of this form to yield accurate values for the region in parameter space in ξ and b of interest here.

Integrals with the R^{-n} asymptotic behavior are more complicated. A sample integral is

$$\int_{-\infty}^{\infty} dz\, e^{iwz}\frac{1}{z^2+b^2}=\frac{\pi}{b}e^{-wb}\,. \tag{16}$$

This integral, with an upper limit of $z=24$, is in general not close to its correct value. The remainder of the integral from $z=24$ to $z=\infty$ is evaluated by deforming the contour, which extends along the real axis to infinity, up the imaginary axis at $z=24$ to a point beyond which there is no further contribution to the integral. The remaining portions of the integral (e.g., parallel to the real axis to infinity) are vanishingly small. That portion of the integral along the imaginary axis converges very well, but care must be exercised because its value in extreme cases (low ξ and large b) is nearly equal in magnitude to, but of opposite sign from, the contribution from the real axis from $z=0$ to $z=24$.

In determining a suitable mesh size in the evaluation of the scattering amplitude, Eq. (11), care was taken of the following. The use of a temporally varying (increasing) binding energy causes a more rapid oscillatory behavior (larger w). The use of a Coulomb trajectory in the repulsive case leads to a decreased projectile velocity v and, hence, to a more rapid oscillation. Finally, the occurrence of final continuum states likewise leads to a larger oscillation rate. It is the numerical accuracy of the evaluations of the integrals of Eqs. (15) and (16) that limits the applicability of calculations of the cross section in practice to values of $\xi \gtrsim 0.17$.

The numerical evaluation of the matrix elements $V^{k,lm}(\mathbf{R}(t))$ was performed at preset values of R. In order to determine $V^{k,lm}(\mathbf{R}(t))$ for values of R in between in the evaluation of the integrals in the variable z, a spline interpolation [42] was performed. This procedure was tested in the evaluation of the integral in Eq. (15). Matrix elements are specific to the target atom and, when polarization is included, to the projectile as well. In practice the matrix elements are stored to save calculational time in studying the energy dependence of the cross section for a given system.

G. Additional considerations

The major thrust of this investigation is the study of the temporal dependence of electron binding and polarization. There are several additional aspects of this problem that have not been included, the most important of which arises from the use of nonrelativistic wave functions. Relativistic effects are known to be important in inner-shell ionization because the velocity of the K-shell electron in targets as light as Cu no longer lies in the nonrelativistic regime. A significant conclusion of this paper will be seen in the observation of a systematic and increasingly larger discrepancy of theory from experiment as the projectile charge Z_P increases. This result can be reached on the basis of the three lightest systems, p and ^{3}He in Ti and ^{6}Li in Cr, and at the highest projectile velocities for which experimental data are available. Under these conditions, relativistic effects are less than 3%. Thus the impact of this (potentially very significant) physical effect on this major conclusion is not a pivotal issue.

It would, nevertheless, be useful and interesting to extend comparisons with data to a broader range of targets in order to infer a possible dependence of the target atomic number and, in particular, on the ratio Z_P/Z_T. In order to include relativistic effects in situations in which this phenomenon is important, the ratio of the relativistic to nonrelativistic total cross section is calculated from the CPSSR [43] model and is incorporated in the calculations of the total cross section reported below as a multiplicative factor. This factor is close to that provided by several other estimates, as summarized by Admunsen, Kocbach, and Hansteen [44] and to the results of calculations performed with relativistic wave functions. Thus, it is felt that meaningful conclusions can be drawn, even though for the worst case considered (0.3 MeV/u ^{6}Li in Pd) the increase in total cross section is 300%. The incorporation of Dirac-Hartree-Fock-Slater wave functions is currently underway.

TABLE I. Values of the total K-shell ionization cross section calculated theoretically with PBBCDP, uncorrected and corrected by the multiplicative factors, ENL and REL from the ECPSSR model for energy loss and relativistic effects for p in Cu and ^{3}He in Ti. These cross sections are denoted by $\sigma^{\mathrm{PBBCDP,u}}$ and σ^{PBBCDP}, respectively. Experimentally measured values, σ^{expt}, are taken from the Paul-Muir reference cross sections [26] for incident protons and from Simons *et al.* [9] for incident ^{3}He ions. All cross sections are given in barns.

System	Energy	$\sigma^{\mathrm{PBBCDP,u}}$	ENL	REL	σ^{PBBCDP}	σ^{expt}
	(MeV)					
$p\rightarrow$Cu	0.2	0.0249	0.868	1.328	0.0287	0.0333
	0.5	1.41	0.946	1.170	1.56	1.62
	1.0	14.7	0.973	1.097	15.7	15.9
	1.5	45.4	0.982	1.065	46.4	48.2
	2.0	90.1	0.987	1.048	93.2	95.7
	(MeV/u)					
^{3}He$\rightarrow$Ti	0.2	2.63	0.971	1.134	2.90	3.15
	0.5	77.3	0.989	1.067	81.5	89.0
	1.0	640.0	0.995	1.034	658.0	787.0
	1.5	1680.0	0.997	1.021	1710.0	2160.0

Another effect that has been neglected involves the energy loss of the projectile in the ionization of the atom. This inherently quantal effect has been estimated from the ECPSSR model [33] and is also included as a multiplicative factor. For incident He and Li this effect is quite small (3% or less); see Table I.

It has been noted that the calculations of the cross sections are performed with a hyperbolic Coulomb trajectory [21]. Details are given in Appendix C.

III. RESULTS OF CALCULATIONS

The present model, characterized by a time-dependent, initial-state binding energy $E_i(t)$ and polarized wave function $\Psi_{\rm pol}(\mathbf{R}(t))$, is now applied in calculations of the total cross section for K-shell ionization. In the following these calculations are denoted by PBBCDP. [PBBCDP is a pseudoacronym, PB standing for $P(b)$, the probability for ionization at impact parameter b, B for binding, C for Coulomb trajectory, and DP for (dipole) polarization.] Results are reported in comparison with the NSWC experimental values of Simons *et al.* [9] for incident protons and He ions and with values measured by Raith, Divoux, and Gonsior [45] for incident Li ions. In all instances involving comparisons with experimental data the present theoretical results are corrected for energy loss and relativistic effects as discussed above.

In Fig. 1 results are shown for incident protons in terms of the ratio of the experimental to the (PBBCDP) theoretical values of cross section as a function of the scaled velocity ξ and cover a range in ξ from 0.4 to 1.2. Targets include Ti, Cr, Ni, and Cu. The agreement between the two is very close, with the theoretical values slightly low ($<10\%$) at the highest values of ξ considered.

In Fig. 2 similar results are shown for incident ^{3}He ions

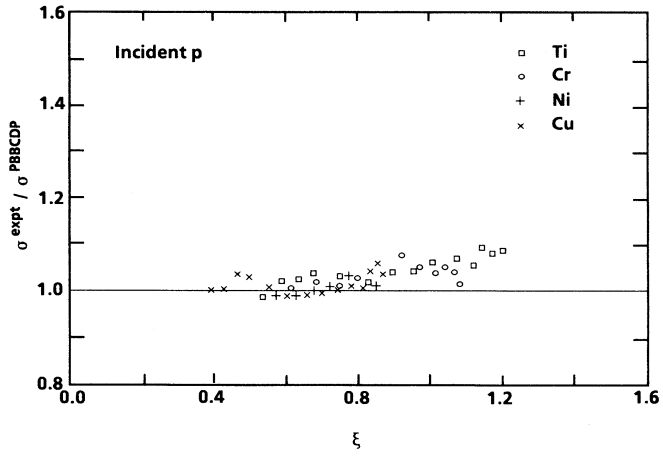

FIG. 1. Ratio of experimental to the PBBCDP theoretical values of the total K-shell ionization cross section as a function of ξ for protons incident on Ti, Cr, Ni, and Cu targets. Energy-loss and relativistic effects are included in the theoretical values from the ECPSSR model [33].

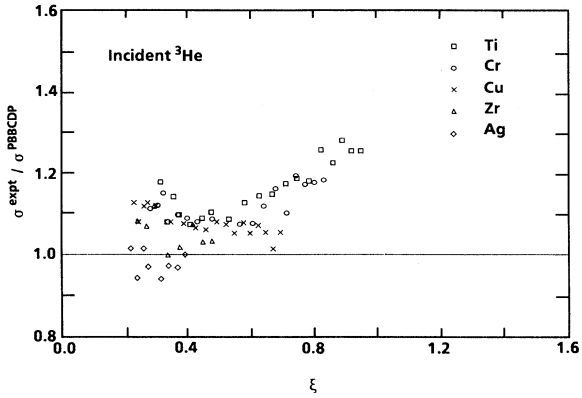

FIG. 2. Same as Fig. 1 for ^{3}He ions incident on Ti, Cr, Cu, Zr, and Ag targets.

in the range of ξ from 0.2 to 1.0. Here somewhat larger discrepancies are noted. The experimental to theoretical ratios for Ti, Cr, and Cu targets are similar, being low by about 10% at low ξ and by 20% at higher ξ. The trend of a larger discrepancy at higher energies, seen for incident protons, is reproduced. For the Zr and Ag targets, there appears, on the average, to be agreement between the theoretical and experimental results. It should be kept in mind that a considerable correction (up to 250%) is required for Zr and Ag targets from relativistic effects. There also is a hint from these results of a dependence of the observed discrepancy on Z_T.

In Fig. 3 comparisons are shown for incident ^{6}Li ions [45]. The range in ξ extends from 0.2 to 1.1. Here discrepancies between theory and experiment are larger still. Also, the trend of larger discrepancies at higher values of ξ continues. However, there is now a clear dependence of the discrepancy on Z_T with smaller differences occurring for larger Z_T. Calculations were also performed for ^{6}Li on Fe ($Z=26$), and the experimental to theoretical ratios lie between those for Cr ($Z=24$)

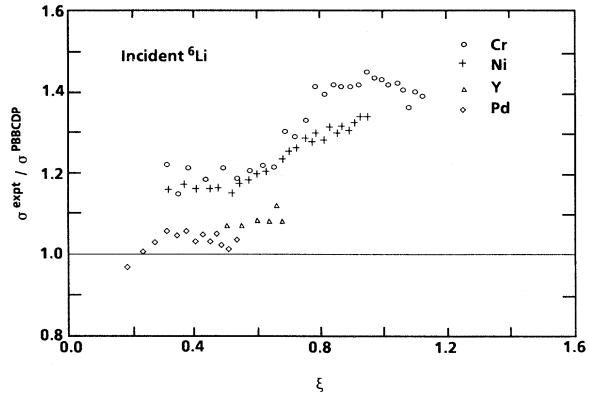

FIG. 3. Same as Fig. 1 for ^{6}Li ions incident on Cr, Ni, Y, and Pd targets.

and Ni ($Z=28$); they are not displayed in the figure for the sake of clarity.

From the above comparisons it is clear that there is a strong dependence of these ratios on Z_P and, from the cases involving incident Li, a manifest dependence on Z_T as well. In order to explore this dependence for incident protons and to extend the domain of comparison between theory and experiment, ratios of the PBBCDP theoretical values to the reference cross sections developed by Paul and Muir [26] are calculated. These reference cross sections, applicable for protons, are based upon a systematic average of many experimental measurements. Since the data considered above cover the region of ξ from roughly 0.2 to 1.2, calculations have been performed in the region from $\xi=0.17$, the minimum value for the reference cross sections, to $\xi=1.2$ for four targets, Al, Ti, Cu, and Ag. The results are displayed in Fig. 4. Here one notes a dependence on Z_T, not present in experimental data limited to the range $22 \leq Z_T \leq 29$. In particular, for higher values of ξ, all the curves rise slightly, in agreement with the overall trend observed above. The different behavior of the curve for Al could arise from coupling effects from the L subshell. At lower ξ the curves exhibit a sharp peak at $\xi \approx 0.275$, below which they fall rapidly.

In Table I some typical numerical values of the total K-shell ionization cross section calculated here along with the contributions from the relativistic and energy loss effects are shown for p in Cu and ^{3}He in Ti.

Calculations of the K-shell cross sections differential in the projectile scattering angle $P(b)$ have also been performed. These are presented in a separate publication [10] in which comparisons with NSWC and other data are shown.

In the development of the present model the incorporation of the time dependence of the binding energy and polarization of the electronic wave function as a function of the position of the projectile was accomplished in two steps. In the first step [20] the temporal dependence of the binding energy alone as a function of the position of the projectile was incorporated with an undistorted wave function. In the second step [25] the time dependence of both the binding energy and a polarized wave function was considered. As discussed above, it was found that the introduction of a time-dependent binding energy with an undistorted wave function gives rise to a large suppression of the total cross section for K-shell ionization at lower velocities; at higher velocities ($\xi \gtrsim 1$) the two cross sections approach one another. However, the introduction of a wave function that is allowed to respond to the time dependence of the projectile position was found to give rise in turn to a large enhancement of the cross section at low ξ that cancels in part the suppression induced by the time-dependent binding.

These results are illustrated in Fig. 5. Two systems are considered, p in Cu and ^{3}He in Ti, spanning values of the ratio Z_P/Z_T from 0.035 to 0.091. The lower curves in each portion of the figure represent the ratio of the cross section calculated with time-dependent binding to that

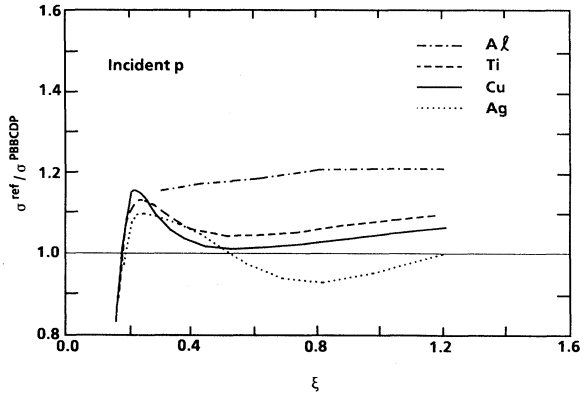

FIG. 4. Ratio of the Paul-Muir reference cross sections [26] to the PBBCDP theoretical values as a function of ξ for protons incident on Al, Ti, Cu, and Ag targets.

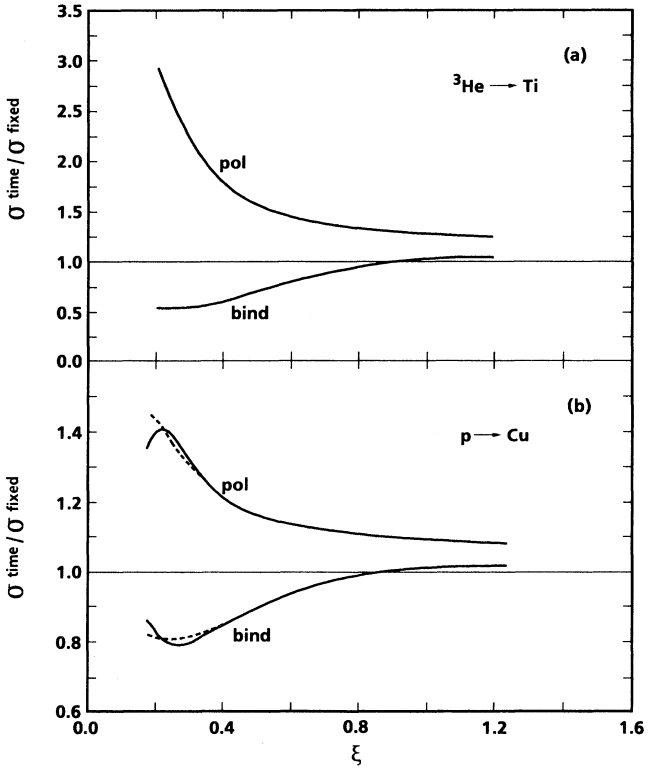

FIG. 5. Ratios of theoretical cross sections as calculated with time-dependent binding (bind) to those calculated with time-independent binding (lower curves) and of cross sections as calculated with time-dependent polarization (pol) to those calculated with time-independent polarization (upper curves) as a function of ξ for ^{3}He in Ti (a) and p in Cu (b). The dashed extrapolations shown for p in Cu represent calculations for a constant-velocity, straight-line trajectory. In this figure and the next, σ^{time} and σ^{fixed} refer to total cross sections calculated with the particular physical effect(s) in question as time dependent or as time independent with $R(t)$ fixed at b.

calculated with the time-independent binding energy evaluated at $R=b$, and demonstrate the significant suppression of the cross section for time-dependent binding. These calculations were performed with an unpolarized wave function. The upper curves represent the ratio of the cross section calculated with time-dependent polarization to those calculated without polarization, and reveal a large enhancement at low ξ. Both of these calculations include temporally dependent binding. As noted above and discussed elsewhere [25], numerical studies of this enhancement showed that its origin is found specifically in the spherically symmetric (monopole) contraction and expansion of the wave function, $\exp[-\zeta(R)r]$, and not in the dipole distortion involving the term with $\lambda(R)$. The latter was found to introduce a shift in the cross section proportional to Z_P/Z_T that is roughly independent of projectile velocity in the velocity region considered here, $\xi \leq 1.2$. It was in order to draw a sharp resolution between these pieces that the wave function of Eq. (2), consisting explicitly of a monopole and dipole part, was introduced as an alternative to the multipole wave function of Eq. (6).

Two additional points should be made in connection with Fig. 5. In the case of p in Cu, the ratios (solid curves) are seen to turn over and approach unity for small ξ, in sharp contrast to the situation involving incident ^{3}He. Most of this behavior arises specifically from the effect of Coulomb deflection in the p-wave part of the amplitude, which is overriding the influence of the temporal dependence of the binding and polarization. To illustrate this, calculations that employ a constant-velocity, straight-line trajectory have also been performed, and the results are indicated by the dashed extrapolations of the solid curves. These ratios are similar to those obtained by ^{3}He in Ti, for which Coulomb effects are considerably weaker because of the heavier mass of ^{3}He. The small rise in the binding curve for incident p at the lowest ξ is starting to be seen for incident ^{3}He also. Secondly, the curves that compare time-dependent versus constant binding rise slightly above unity at large ξ. The naively expected behavior of the cross section in which the binding varies between two limits is that its value would lie between values appropriate for the limiting cases. This clearly does not happen except at large ξ.

The ratios shown in Fig. 5 that include polarization exhibit the enhancement at low velocity just described, but differ from unity at high velocity because of the total neglect of polarization in the calculated cross sections of the denominators. In order to see the effect of a "time-independent" polarized wave function, the following calculations were additionally performed. In the polarized wave function of Eq. (2), the value of R in the monopole portion, $R_B(r,\zeta(R))$, was taken in the united-atom limit, i.e., at $R=0$. This gives rise to a time-independent monopole piece. However, in order to maintain compatability with existing computer codes, the time dependence of R was kept in the dipole term involving $\lambda(R)$. It has been shown [25], as remarked above, that the temporal dependence of the dipole portion does not contribute to the large enhancement at low velocity. Thus, the polarized wave function just described is appropriate to illustrate the effect of time independent polarization.

The results of these calculations are shown in Fig. 6. The lower curves represent time-dependent versus time-independent binding and are taken from Fig. 5 for comparison. With respect to these ratios, it should be noted that corresponding calculations performed with time-independent polarization as described above are indistinguishable from those shown. The upper curves represent the ratio of the total cross section calculated with the full temporally dependent wave function of Eq. (2) (PBBCDP) to those calculated with the monopole portion evaluated in the united-atom limit. The enhancement at low velocities, though not as large as that seen in Fig. 5, is still quite pronounced. In addition, the ratios are close to unity at the higher velocities, as would be expected. The middle pair of curves represents the ratio of cross section calculated with complete time dependence of both polarized wave function and binding energy (PBBCDP) to those calculated with the time-independent monopole portion of initial-state wave and time-independent binding. While these curves show a modest structure, they are near unity, suggesting some cancellation at the lowest velocities considered in the figure between the enhance-

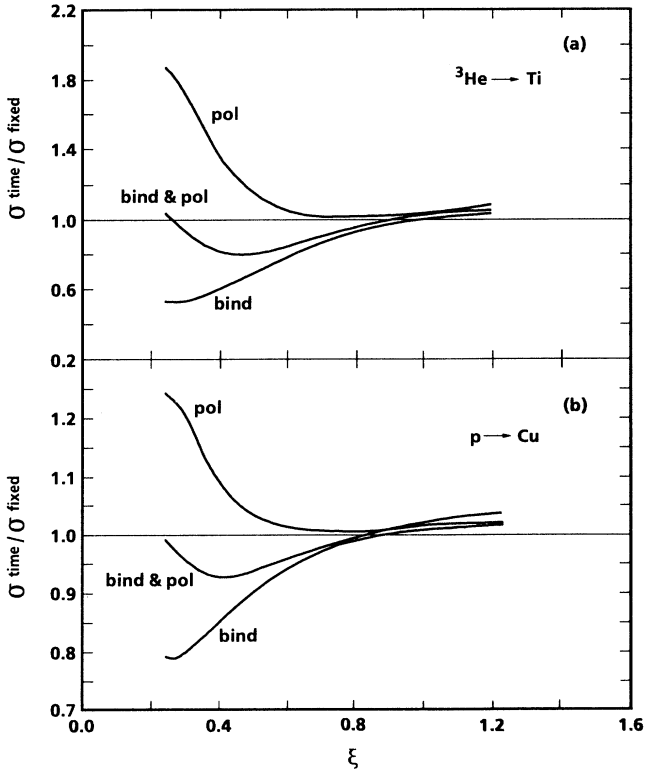

FIG. 6. Ratios of theoretical cross sections as calculated with time-dependent effects to those with time-independent effects as a function of ξ for ^{3}He in Ti (a) and p in Cu (b). The lower curves represent the effect of binding, the upper curves the effect of polarization, and the middle curves the effects of both binding and polarization.

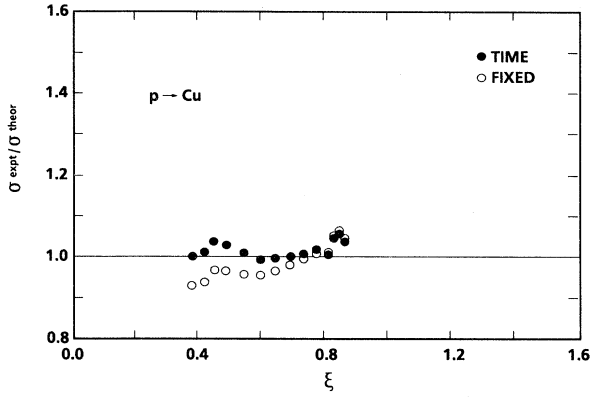

FIG. 7. Ratios of experimental values to the theoretical values calculated with time-dependent binding and polarization (PBBCDP) and with time-independent binding and polarization of the total K-shell ionization cross section as a function of ξ for p in Cu. Energy-loss and relativistic effects are included in the theoretical values from the ECPSSR model [33].

ment and suppression occurring from temporal dependence of the polarization and binding, respectively, and illustrate the situation that past calculations which neglect the time dependence of the binding energy and wave function distortion have often shown reasonable agreement with experiment. The results of Ref. 4 provide a good example for low-velocity incident projectiles.

Having introduced time-dependent binding and polarization, and having seen that discrepancies with experimental data remain, has anything been gained over evaluating these quantities at some fixed time? To answer this question, let us confront each calculation with experimental data. This is done in Figs. 7–9 for p in Cu and ^{3}He in Ti and also for ^{6}Li in Cr. Data are from Ref. [9] for p and ^{3}He and Ref. [45] for ^{6}Li. For p in Cu both calculations are generally to within 5% of the data, although the calculations having full time dependence are in a little closer agreement overall. The remaining two systems exhibit trends that are quite similar. Calculations with the full time dependence lie below the experimental values, with the discrepancy increasing for higher velocities, as shown in Figs. 2 and 3. Those calculations performed with binding and polarization time independent are close to the time-dependent results at higher velocities, as would be expected, but at lower velocities exhibit a pronounced and (perhaps) undesirable structure with a large dip near $\xi \approx 0.4$. While on the average the time-independent results are closer to experiment, the absence of structure in the ratio that follows from the use of time-dependent binding and polarization appears more persuasive in favoring this model with respect to comparison with data.

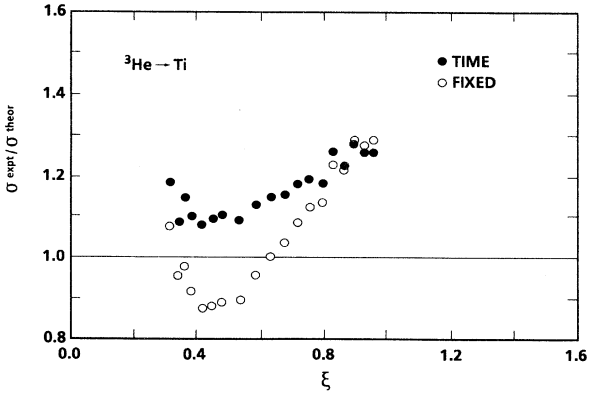

FIG. 8. Same as Fig. 7 but for ^{3}He in Ti.

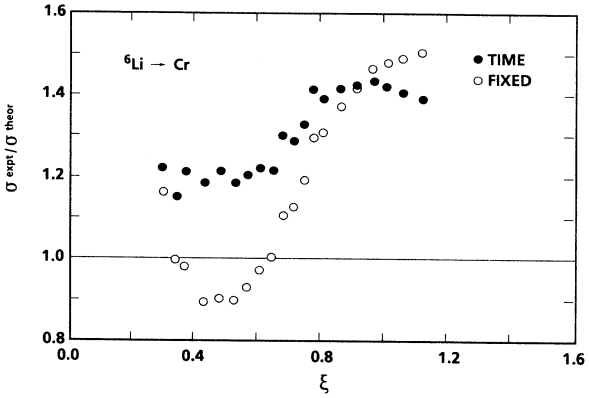

FIG. 9. Same as Fig. 7 but for ^{6}Li in Cr.

Figure 10 shows comparisons in the cross sections for the two forms of polarized wave function discussed above, the dipole wave function Eq. (2) and the multipole wave function Eq. (6). Two systems are considered, p in Cu and ^{3}He in Ti. The multipole wave function, whose calculations are denoted by PBBCPL, gives rise to some-

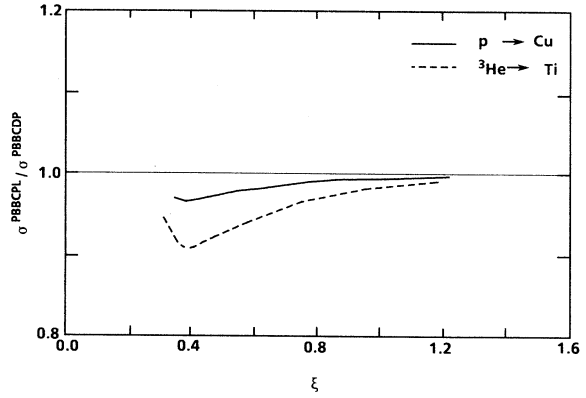

FIG. 10. Ratio of values of the cross section calculated with the multipole wave function, Eq. (6), (PBBCPL) to those calculated with the dipole wave function, Eq. (2), (PBBCDP) as a function of ξ for p in Cu and ^{3}He in Ti.

what lower values of total cross section with the difference increasing with larger Z_P/Z_T, as would be expected. While the largest difference of nearly 10% is seen for the ^{3}He projectile in Ti at $\xi=0.4$, the overall similarity between the results of the two wave functions gives credence to the use of either to characterize the effects of wave-function distortion.

Calculations in configuration space of the matrix elements of the potential with the multipole wave function proceed in a similar way to those without polarization. In addition to the expansion of the $1/|\mathbf{r}-\mathbf{R}|$ part of the potential in spherical harmonics, Eq. (12), the contribution from polarization can readily be included through an analogous expansion in spherical harmonics of the product $\exp(-Z_P|\mathbf{r}-\mathbf{R}|)/|\mathbf{r}-\mathbf{R}|$ [46], which combines the polarized piece of the wave function with the electron-projectile potential.

IV. MATHEMATICAL ANALYSIS OF TIME-DEPENDENT BEHAVIOR

With such dramatic changes in the scattering amplitude upon the introduction of time-dependent binding or polarization as observed in Fig. 5, it is of interest to understand their origin. In previous work [20] a study was performed to determine the cause of the large suppression of the scattering amplitude at low projectile velocities when the electron binding energy is allowed to depend on time. This study proceeded through an analysis by the method of steepest descent of integrals prototypical of those that occur in the expression for the scattering amplitude, Eq. (11). Here this analysis is extended to include a time-dependent monopole moment of the type that was found responsible for the observed enhancement. It should be emphasized that this analysis is intended as qualitative in nature; details depend on the exact form of the assumed matrix element of V. In this section as in Sec. II F, the unit of length is the K-shell radius $1/Z_{TK}$.

The scattering amplitude of Eq. (11) may be expressed generically in the form

$$I=\int_{-\infty}^{\infty} dz \exp\left[i\frac{\omega}{v}z+\frac{i}{v}\int_0^z dz'\Delta E(R')\right]V(R) , \tag{17}$$

where $V(R)$ represents the matrix element of the potential and $\Delta E(R)$ is given by $[E_i(t)-\frac{1}{2}]$ from Eq. (3). A temporally dependent binding energy is thus explicitly included. Here R is given by $(b^2+v^2t^2)^{1/2}$, implying a straight-line trajectory. Several forms of $V(R)$ were studied previously [20] and the form most amenable for the present analytic consideration is $V(R)=\exp(-R)$. Here, in order to incorporate temporally varying polarization, the function $V(R)$ is generalized to

$$V(R)=\zeta(R)^{3/2}e^{-\zeta(R)R} ,$$

where $\zeta(R)$ is the effective charge factor defined in Eq. (4).

An integral of the form

$$I(s)=\int dz\, e^{s f(z)} \tag{18}$$

may be approximated for large s by [47]

$$I(s)\cong\frac{\sqrt{2\pi}e^{sf(z_c)}e^{i\alpha}}{|sf''(z_c)|^{1/2}} . \tag{19}$$

Here z_c is the location of a zero of $f'(z)$, which is a genuine saddle point (in general, a sum must be taken over all saddle points) and α is the angle such that $f''(z_c)(z-z_c)^2e^{2i\alpha}$ is real and negative. The function $f(z)$ in the present instance has a singular point, and the significant issue will be the relative location of the critical point z_c to the singular point in $f(z)$ since $f''(z_c)$ is sensitive to z_c.

The model amplitude defined by Eq. (17) clearly is of the form of Eq. (18), in which

$$s=\omega/v\equiv w ,$$

$$f(z)=iz-\frac{R}{w}+\frac{i}{\omega}\int_0^z dz'\Delta(R(z'))$$
$$-\frac{1}{w}\Delta\zeta(R)R+\frac{3}{2w}\ln\zeta(R)$$
$$\equiv g(z)+h(z) ,$$

where

$$g(z)=iz-R/w ,$$

and $h(z)$ is the remaining portion of $f(z)$, which is of the order of Z_P/Z_T. $w=\omega/v$ is assumed large. $\Delta\zeta(R)$ is given in analogy with the definition of $\Delta E(R)$ by $[\zeta(R)-1]$. Note that $f(z)$ is singular at $z=\pm ib$.

The critical point of $f(z)$, z_c, is obtained from $f'(z_c)=0$. For $h=0$, the critical point of $g(z)$, z_c', is readily found to be

$$z_c'=\frac{iwb}{(1+w^2)^{1/2}} ,$$

which lies below the singular point at $z=+ib$ and is the only saddle point. The critical point of $f(z)$ may be found perturbatively. From $f'(z_c)=0$, one finds

$$0=i-\frac{1}{w}\frac{z_c}{(z_c^2+b^2)^{1/2}}+\frac{dh(z_c)}{dz} ,$$

or, upon squaring,

$$-w^2(z_c^2+b^2)=z_c^2-2wz_c(z_c^2+b^2)^{1/2}\frac{dh(z_c)}{dz}$$
$$+O(Z_P/Z_T)^2 .$$

If it is assumed that z_c differs from z_c' by terms of the order of Z_P/Z_T, then z_c may be replaced by z_c' everywhere in the term involving dh/dz, provided that dh/dz remains bounded near the singular point at $z=ib$. One finds that

$$\frac{dh}{dz}=\frac{i}{\omega}\Delta(R)-\frac{1}{w}\frac{dR}{dz}\left[\Delta\zeta(R)+\left[1-\frac{3}{2}\frac{1}{\zeta}\right]\frac{d\zeta}{dR}\right] .$$

Under the stated assumptions, one has $R(z_c)\approx 0$ and $dR(z_c)/dz\approx iw$. Thus, $dh(z_c)/dz$ is bounded. Further-

more, at $R=0$, $d\zeta/dR$ is zero, and $\Delta(R)$ and $\zeta(R)$ both have the value Z_P/Z_T. Thus, correct through order of Z_P/Z_T, the critical point z_c is given by

$$z_c \approx \frac{ibw}{(w^2+1)^{1/2}}\left[1+\frac{Z_P}{Z_T}\frac{1}{w^2+1}\left[\frac{1}{\omega}-1\right]\right]. \quad (20)$$

The term involving the second derivative $f''(z_c)$ in Eq. (19) is found to be

$$|sf''(z_c)|^{-1/2} \approx \frac{b^{1/2}}{(w^2+1)^{3/4}}\left[1-2\frac{Z_P}{Z_T}\left[\frac{1}{\omega}-1\right]\right]^{3/4}. \quad (21)$$

In these expressions the terms associated with binding and polarization are the factors within the parentheses $1/\omega$ and unity, respectively. The critical point always remains below the singular point. The effect of binding is to move the critical point nearer the singular point, while the effect of polarization is to move the critical point away from the singular point and by a comparable amount.

We note an important result from these expressions. While the shift in the location of the critical point arising from binding and polarization is of the order of $(Z_P/Z_T)/w^2$, a very small quantity because w is assumed large, the change in the value of f'' is of the order of Z_P/Z_T, which is much larger. This difference occurs because of the singularity in $f(z)$ at $z=ib$, and emphasizes the sensitivity of the value of the integral to the location of the critical point.

In the case in which binding and polarization are evaluated at the distance of closest approach such that $\Delta(R)$ and $\zeta(R)$ take the constant values $\Delta(b)$ and $\zeta(b)$, Eqs. (20) and (21) are replaced by

$$z_c = \frac{ibw}{(w^2+1)^{1/2}}\left[1+\frac{1}{w^2+1}\left[\frac{\Delta E(b)}{\omega}-\Delta\zeta(b)\right]\right]$$

and

$$|sf''(z_c)|^{-1/2} = \frac{b^{1/2}}{(w^2+1)^{3/4}} \times \left[1-2\left[\frac{\Delta E(b)}{\omega}-\Delta\zeta(b)\right]\right]^{3/4}.$$

Here the shift in the location of the critical points is smaller than when the binding energy or wave-function polarization is allowed to vary with projectile position. $\Delta E(R)$ and $\Delta\zeta(R)$ are evaluated at $R=b$ rather than at $R=0$, where they are smaller in magnitude. Thus, the overall effect on the scattering amplitude from each is expected to be significantly smaller.

In this example the actual change in the scattering amplitude arising from the time-dependent treatment of binding and/or polarization is seen to be rather small, of the order of Z_P/Z_T, which is perturbative in nature. However, the earlier study [20] of binding alone showed that detailed results depend strongly on the form of $V(R)$. The specific case of $V(R)$ given by $(1+R)\exp(-R)$, a case not so readily tractable to analysis, was shown numerically to lead to a large suppression of the amplitude. This suppression is larger than what is obtained from using for $V(R)$ an actual matrix element of the potential, Eq. (13), for zero-energy outgoing electrons, as an example. Another case was studied in which a 0 developed in the amplitude.

In summary, the analysis of the integral of Eq. (17) with $V(R)$ given by $\zeta(R)^{3/2}\exp[-\zeta(R)R]$ shows that its value for large w is dominated by the location of a critical point relative to the location of a singular point, and that the shift in the location of the critical point is larger for the case of time-dependent binding and/or polarization than for constant binding and/or polarization. For binding, the shift is towards the singularity, and for polarization it is away from the singularity. Because of the occurrence of the factor $|f''(z_c)|^{-1/2}$ in Eq. (19), the value of the integral is suppressed for binding or enhanced for polarization, and this change is exaggerated because of the nearby singularity in $f(z)$. Recall that ω is given by $E_f-E_i \geq \frac{1}{2}$. The shift in location of the singular point is of comparable magnitude for binding and polarization but is not the same. The effects of binding and polarization do not necessarily cancel.

V. DISCUSSION

The comparisons between experiment and theory presented above reveal systematic discrepancies that increase as Z_P increases and appear to decrease as Z_T increases. Since the ratio Z_P/Z_T is fundamental in the theory, it could be asked whether these discrepancies are consistent with a dependence on this ratio. It should be noted that Z_P/Z_T ranges from about 0.02 for p in Ag to 0.13 for Li in Cr, covering a range of about 6. A systematic dependence on Z_P/Z_T of the discrepancy in the ratios of experimental to theoretical cross sections would translate to a systematic dependence on $(Z_P/Z_T)^n$ of the error in the amplitudes $b_f(\infty)$, where n is most likely 2 or 3. [Recall that $b_f(\infty)$ already contains terms of the order of Z_P/Z_T in lowest order.] As the ratios now stand, such a dependence is not clear. However, if these ratios were increased by about 10% (i.e., theory decreased by 10%), then one would find a rough proportionality between these increased ratios minus unity and Z_P/Z_T, implying an error of the order of $(Z_P/Z_T)^2$ in the amplitude. For p in Cu this error would be about 5–7 %. This certainly is not unreasonable.

One might speculate on the origin of a constant shift of these ratios from reported calculations of Ford, Fritchard, and Reading [6]. These authors had introduced the use of Hartree-Fock wave functions, including an accurate treatment of the exchange term, into the problem in proton-induced K-shell ionization and contrasted these results (in the Born approximation) with those obtained with screened hydrogenic wave functions employed here. Cross sections obtained with Hartree-Fock wave functions were found to be about 10% lower than those obtained with screened hydrogenic wave functions. This property relates to a Z_T dependence and could be roughly independent of Z_p. Thus the use of

more accurate wave functions, such as Hartree-Fock wave functions or, more elaborately, wave functions that include the configuration interaction, could account for a shift in these ratios.

There are several possible origins for error of the order of $(Z_P/Z_T)^2$. The polarized wave function employed here to describe the behavior of the initial-state electron is clearly only an approximation. The nature of the approximation can be appreciated if it is recalled that Eq. (11) would represent an exact expression for the scattering amplitude in the post form if the wave function $\Psi_{\rm pol}(t)$ were replaced by $\Psi^{(+)}(t)$, the exact solution of the Schrödinger equation satisfying the boundary condition $\Psi^{(+)}(t)\rightarrow\phi_i \exp(-iE_i t)$ as $t\rightarrow-\infty$ (with due account being given to an $\exp(-iE_f t)$ factor). In addition, no distortion of the ejected electron (final-wave function) is considered, either explicitly in terms of a ψ_f in the two-state approximation or implicitly in terms of a more accurate description of an assumed $\Psi^{(+)}$. In this regard it would be quite interesting to employ the variationally developed wave function of Kleber and Unterseer [31] as a particularly appropriate approximation for $\Psi^{(+)}$; distortion of both initial and final states is implicitly included in this approach.

And there is a subtle source of error. In the perturbation theory used in the calculations, a unitary transformation, Eq. (8), is introduced to remove diagonal terms from the right-hand side of the equations for the amplitude. This transformation, from which the binding effect follows, appears as a multiplicative factor in both the monopole and dipole terms of the initial-state wave function. But in a derivation intended to motivate the presence of this factor at low velocities, Reading [48] has shown, from a consideration of a class of terms in the Born series, that this factor is associated with only the unperturbed part of the initial-state wave function. It would follow that, from the point of view of an expansion of this term in Z_P/Z_T, only portions of it would multiply the polarized parts of an initial-state wave function. This includes both dipole *and* monopole parts. Thus, errors of this type appear in the amplitude to order $(Z_P/Z_T)^2$. This point should be kept in mind in the application of approximation schemes such as the perturbation theory employed here [Eq. (10)] or the two-state approximation or the method of symmetric orthogonalization discussed above. These methods might not be sufficiently accurate for reliable solutions.

Another source of discrepancy between theory and experiment is the omission of the contribution from the capture of the K-shell electron by the projectile. This cross section is always included in the experimental measurements. Estimates of its magnitude can be made on the basis of the strong potential Born theory of Macek and Alston [49] with the inclusion of K-shell binding. For a Cr target the contribution is negligible for incident protons, but it is of the order of 5% for ^{3}He ions and 20% for ^{6}Li ions. This magnitude, especially for Li, partially negates the arguments made above relating the dependence of the observed discrepancies on Z_P/Z_T. However, application of this theory to p in Ne, a system having a similar Z_P/Z_T and Z_T/v as Li on Cr, predicts electron capture cross sections that are twice as large as values measured by Rodbro *et al.* [50]. The estimates for Li in Cr could also be large. Thus, electron capture undoubtedly plays a role, but the main thrust on the conjecture on the origin of the observed systematic differences between theory and experiment outlined above should still hold.

All calculations presented here have been performed under the assumption that the K-shell electron responds instantaneously to the motion of the projectile. This is the basis of adiabatic perturbation theory, which is indeed to apply at very low velocities, $\xi\rightarrow0$, and which formed the motivation [16, 51] of this work. The calculations here extend to $\xi\approx1.2$. It would be expected that there should be some breakdown of this approximation at these velocities. A study of this issue [52], which rests on a variational principle [53] designed to minimize the effects of coupling to higher states, has been performed. Results were presented by showing the behavior of the effective charge of the target nucleus as perceived by the K-shell electron $\zeta(t)$ as a function of projectile position for several projectile velocities from $\xi=0$ to 50. These results generalize that given for $\zeta(t)$ in Eq. (4), which is appropriate for ξ close to zero. It was found that, for $\xi=1$, $\zeta(t)$ is sufficiently close to its values for $\xi=0$ that the difference is not significant. For $\xi=50$, $\zeta(t)$ is close to unity for all t, thereby implying the Born approximation, in which the wave function does not respond at all to the motion of the projectile. The effect of the transition from the adiabatic to the nonadiabatic region in the present calculations remains a consideration for future work.

In connection with this point, it is interesting to draw a distinction between the K-shell electron binding energy and velocity for the projectile located at the target nucleus, $R=0$. The use of Eq. (3) for the binding energy does not strictly correspond to the binding energy in the united-atom limit: it predicts a larger binding. The reason for this choice, also discussed in Ref. [52], was that the outer electrons of the target atom are largely unperturbed by the passage of the projectile. Hence, no change in outer screening is introduced, and the binding energy of the K-shell electron is larger than that for a nucleus having $Z=Z_T+Z_P$. On the other hand, the use of Eq. (4) for the effective charge $\zeta(t)$ does imply the K-shell electron velocity exactly in the united-atom limit. The electron velocity is directly related to its wave function, which, as just discussed, is treated in the adiabatic limit.

I conclude with a remark on the introduction of temporally dependent quantities in approximate theoretical descriptions, such as the present one. It has been shown that the occurrence of such time-dependent factors can lead to large changes in the scattering amplitude, and, hence, in the cross section. In the present model, a large suppression of the amplitude caused by time-dependent binding is cancelled in part by a large enhancement caused by time-dependent polarization. The observations of the preceding paragraph, in which the quantity $\zeta(t)$ is associated with the electron velocity, might suggest that if the electron energy is treated in a time-dependent way, the electron velocity must be similarly treated. This im-

plies the temporal dependence of the monopole moment; i.e., a time-dependent polarization. The mathematical analysis discussed in Sec. IV suggests that exact cancellation is not implied. It would, therefore, seem prudent to exercise caution in the use of temporally dependent quantities in approximate calculations. Nevertheless, it appears from Figs. 7–9 that the time-dependent approach does yield a more stable behavior of the theoretical cross sections in comparison with experimental data. Also, the approach of utilizing approximate analytic wave functions contains the possibility of including classes of terms to all orders in Z_P/Z_T and allows the advantage of obtaining additional physical insight.

ACKNOWLEDGMENTS

The author thanks Dr. George Basbas for initiating these studies and for numerous discussions. He is especially grateful to Professor John Reading of Texas A&M University for many beneficial discussions over a period of several years. He thanks Professor Helmut Paul for several helpful discussions and Professor William Thompson of the University of North Carolina for providing the computer algorithm to calculate the spline interpolation in these calculations. This work was supported by the Independent Research Program of the Naval Surface Warfare Center.

APPENDIX A

The parameter $\lambda(R)$ in $\Psi_{\rm pol}$ is determined by minimizing the total energy $E_i(t)$ with ζ fixed. With λ nonzero, Eq. (3) generalizes to

$$E_i(t)=(\Psi_{\rm pol},H(t)\Psi_{\rm pol})$$
$$=N(R)^2\left\{-\frac{\zeta^2}{2}+\left[1+\frac{1}{2}\left[\frac{\lambda}{\zeta}\right]^2\right]\left[1-\frac{Z_{TK}}{\zeta}\right]^2\zeta^2 - \frac{Z_P}{R}\left[v_1(R)+\frac{\lambda}{\zeta}\frac{2}{\zeta R}v_2(R)+\left[\frac{\lambda}{\zeta}\right]^2\frac{3}{\zeta^2R^2}v_3(R)+\left[\frac{\lambda}{\zeta}\right]^2 v_4(R)\right]\right\}.$$

Here,

$$v_1(R)=1-e^{-2\zeta R}(1+\zeta R)\,,$$
$$v_2(R)=1-e^{-2\zeta R}(1+2\zeta R+2\zeta^2R^2+\zeta^3R^3)\,,$$
$$v_3(R)=1-e^{-2\zeta R}(1+2\zeta R+2\zeta^2R^2+\tfrac{4}{3}\zeta^3R^3 +\tfrac{2}{3}\zeta^4R^4+\tfrac{2}{9}\zeta^5R^5)\,,$$
$$v_4(R)=1-e^{-2\zeta R}(1+\tfrac{3}{2}\zeta R+\zeta^2R^2+\tfrac{1}{3}\zeta^3R^3)\,.$$

E_i can be put into the form

$$E_i=\frac{A+(\lambda/\zeta)B+(\lambda/\zeta)^2C}{1+(\lambda/\zeta)^2}\,,$$

where

$$A=-\frac{\zeta^2}{2}+\left[1-\frac{Z_{TK}}{\zeta}\right]\zeta^2-\frac{Z_P}{R}v_1(R)\,,$$
$$B=-\frac{Z_P}{R}\frac{2}{\zeta R}v_2(R)\,,$$
$$C-\frac{1}{2}\left[1-\frac{Z_{TK}}{\zeta}\right]\zeta^2-\frac{Z_P}{R}\left[\frac{3}{\zeta^2R^2}v_3(R)+1\right]\,.$$

The extremum of E_i is obtained when λ/ζ is given by

$$\frac{\lambda}{\zeta}=\frac{[(C-A)^2+B^2]^{1/2}-(C-A)}{-B}\,.$$

For the asymmetric case, $Z_P\le 0.3Z_{TK}$, A is of the order of Z_{TK}, while B and C are of the order of Z_P. Then one may set

$$\frac{\lambda}{\zeta}\approx\frac{1}{2}\frac{-B}{C-A}\approx 2\frac{Z_P}{\zeta(\zeta R)^2}v_2(R)\,,$$

which is Eq. (5).

APPENDIX B

For completeness, the following relations, which facilitate the evaluations of Eqs. (13) and (14), are noted [40]. In terms of the standard 3-j symbol,

$$\begin{pmatrix} l & l' & l'' \\ m & m' & m'' \end{pmatrix}\,,$$

the integral over all solid angles for the product of three spherical harmonics is given by

$$\int d\Omega_r Y^*_{lm}(\hat{\mathbf{r}}) Y_{l'm'}(\hat{\mathbf{r}}) Y_{1m''}(\hat{\mathbf{r}})$$
$$= (-1)^m \left[\frac{(3(2l+1)(2l'+1)}{4\pi} \right]^{1/2} \times \begin{bmatrix} l & l' & 1 \\ 0 & 0 & 0 \end{bmatrix} \begin{bmatrix} l & l' & 1 \\ -m & m' & m'' \end{bmatrix} .$$

The required orthogonality relation for the 3-j symbols reads

$$\sum_{m'm''} \begin{bmatrix} l' & 1 & l \\ m' & m'' & -m \end{bmatrix} \begin{bmatrix} l' & 1 & \bar{l} \\ m' & m'' & \bar{m} \end{bmatrix} = \frac{1}{2l+1} \delta_{l\bar{l}} \delta_{-m,\bar{m}} \delta(l',1,l) ,$$

where $\delta(l',l'',l)$ equals 1 if l', l'', and l satisfy the triangular condition, and is zero otherwise. Finally, the following specific 3-j symbols occur:

$$\begin{bmatrix} l & l-1 & l \\ 0 & 0 & 0 \end{bmatrix} = (-1)^l \left[\frac{l}{(2l-1)(2l+1)} \right]^{1/2} ,$$

$$\begin{bmatrix} l & l+1 & 1 \\ 0 & 0 & 0 \end{bmatrix} = (-1)^{l+1} \left[\frac{l+1}{(2l+1)(2l+3)} \right]^{1/2} .$$

APPENDIX C

The Coulomb trajectory is characterized by the parametric equations [54]

$$z = S_0 \sinh\Omega [(\epsilon-1)/(\epsilon+1)]^{1/2} , \quad \text{(C1)}$$

$$y = S_0 (\cosh\Omega + \epsilon)/(\epsilon+1) , \quad \text{(C2)}$$

$$R = S_0 (\epsilon \cosh\Omega + 1)/(\epsilon+1) , \quad \text{(C3)}$$

$$t = S_0 (\epsilon \sinh\Omega + \Omega)/[(\epsilon+1)v] , \quad \text{(C4)}$$

in which S_0 is the distance of closest approach, ϵ is the eccentricity parameter given by

$$\epsilon = \frac{1+(b/S_0)^2}{1-(b/S_0)^2} ,$$

and Ω is a parameter. S_0 can be found from b by

$$S_0 = d + (b^2+d^2)^{1/2} ,$$

where d is half the distance of closest approach for a head-on collision,

$$d = \frac{e^2 Z_P Z_T}{M_R v^2} .$$

M_R is the reduced mass for the projectile-target system.

The basic expression for the scattering amplitude, Eq. (11), is given in terms of an integration over time. Equations (C1) and (C4) can be combined to yield

$$t = \frac{1}{v} \frac{\epsilon}{\epsilon+1} \frac{S_0}{b} \left\{ z + \frac{b}{\epsilon} \ln \left[\frac{z}{b} + \left[\frac{z^2}{b^2} + 1 \right]^{1/2} \right] \right\} ,$$

$$dt = \frac{1}{v} \frac{\epsilon}{\epsilon+1} \frac{S_0}{b} \frac{1}{1-(S_0/R)(\epsilon+1)} dz .$$

These are the relations used in the evaluation of the scattering amplitude. Notice that the effect of the Coulomb trajectory is to replace the factor ω/v in the exponential $\exp(i\omega/vz)$ occurring in the scattering amplitude by $\omega/v\, S_0/b$. Thus the rate of oscillation of the integrand is increased by the factor S_0/b near $t=0$.

[1] P. D. Fainstein, V. H. Ponce, and R. Rivarola, J. Phys. B **21**, 287 (1988); **21**, 2989 (1988).
[2] J. F. Reading and A. L. Ford, Phys. Rev. Lett. **58**, 543 (1987); J. Phys. B **20**, 3747 (1987).
[3] H. Knudsen, Nucl. Instrum. Methods B **42**, 536 (1989).
[4] J. M. Hansteen, L. Kocbach, and A. Graue, Phys. Scripta **31**, 63 (1985).
[5] D. J. Land, Nucl. Instrum. Methods A **240**, 470 (1985).
[6] A. L. Ford, E. Fritchard, and J. F. Reading, Phys. Rev. A **16**, 133 (1977).
[7] H. Paul, Nucl. Instrum. Methods B **42**, 443 (1989).
[8] G. Mehler, W. Greiner, and G. Soff, J. Phys. B **20**, 2787 (1987).
[9] D. G. Simons, J. L. Price, D. J. Land, and M. D. Brown, Phys. Rev. A **39**, 3884 (1989).
[10] D. G. Simons, D. J. Land, M. D. Brown, and C. L. Cocke, Phys. Rev. A **42**, 1324 (1990).
[11] J. Bang and J. M. Hansteen, K. Dan. Vidensk. Selsk. Mat.-Fys. Medd. **31**, No. 13 (1959).
[12] J. M. Hansteen, Nucl. Instrum. Methods B **42**, 426 (1989).
[13] W. Brandt, R. Laubert, and I. Sellin, Phys. Rev. **151**, 56 (1966).
[14] G. Basbas, W. Brandt, and R. Laubert, Phys. Rev. A **7**, 983 (1973).
[15] G. Basbas, W. Brandt, and R. Laubert, Phys. Rev. A **17**, 1655 (1978).
[16] G. Basbas, W. Brandt, and R. H. Ritchie, Phys. Rev. A **7**, 1971 (1973).
[17] D. R. Bates, Proc. R. Soc. London **73**, 227 (1959).
[18] E. C. Goldberg and V. H. Ponce, Phys. Rev. A **22**, 399 (1980).
[19] L. Kocbach, Nucl. Instrum. Methods B **4**, 248 (1984); T. Mukoyama and C. D. Lin, Phys. Rev. A **40**, 6886 (1989).
[20] D. J. Land, Nucl. Instrum. Methods B **27**, 491 (1987).
[21] O. Aashamar and L. Kocbach, Z. Phys. A **279**, 237 (1976); J. Phys. B **10**, 869 (1977); G. L. Swafford, J. F. Reading, A. L. Ford, and E. Fitchard, Phys. Rev. A **16**, 1329 (1977).
[22] E. Laegsgaard, J. U. Andersen, and M. Lund, in *Proceedings of the 10th International Conference on Physics of Electronic and Atomic Collisions (Paris)*, edited by G. Watel (North-Holland, Amsterdam, 1978), p. 353; J. U. Andersen, E. Laegsgaard, and M. Lund, Nucl. Instrum. Methods **192**, 79 (1982).
[23] D. J. Land, G. Basbas, M. D. Brown, and D. G. Simons, IEEE Trans. Nucl. Sci. **NS-30**, 1103 (1983).
[24] G. Basbas and D. J. Land, Phys. Rev. A **35**, 1003 (1987).

The calculations reported in this reference were performed under the approximation of a static initial-state wave function polarized by a fixed projectile positioned at its distance of closest approach to the target nucleus. However, a factor necessary for the correct implementation of this model was inadvertently treated as a δ function in the calculations. These calculations, nevertheless, can be shown to possess a sound physical interpretation in terms of a polarized wave function that has a time-dependent dipole moment similar to that given by Eq. (5) of the present paper and a monopole moment that is only weakly dependent upon $R(t)$, unlike the dependence implied by Eq. (4) of the present paper. The resolution of this development and the presentation of comparisons of the original calculations with the present ones are planned to be treated elsewhere.

[25] D. J. Land, Nucl. Instrum. Methods B **42**, 436 (1989).
[26] H. Paul and J. Muir, Phys. Rep. **135**, 47 (1986).
[27] D. Trautmann and Th. Kauer, Nucl. Instrum. Methods B **42**, 449 (1989).
[28] E. Merzbacher and H. W. Lewis, in *Corpuscles and Radiation in Matter II,* Vol. 34 of *Handbuch der Physik,* edited by S. Flügge (Springer-Verlag, Berlin, 1958), p. 166.
[29] P. A. Amundsen, J. Phys. B **11**, 3197 (1978); M. Kleber and K. Unterseer, Z. Phys. A **292**, 311 (1979); F. Rosel, D. Trautmann, and G. Bauer, Nucl. Instrum. Methods **192**, 43 (1982).
[30] A. Temkin, Phys. Rev. **116**, 358 (1959).
[31] M. Kleber and K. Unterseer, Z. Phys. A **292**, 311 (1979).
[32] O. Benka, M. Geretschläger, and H. Paul, J. Phys. (Paris) Colloq. **12**, C9-251 (1987).
[33] W. Brandt and G. Lapicki, Phys. Rev. A **23**, 1717 (1981).
[34] D. S. F. Crothers and J. F. McCann, J. Phys. B **16**, 3229 (1983).
[35] L. D. Landau and E. M. Lifshitz, *Quantum Mechanics* (Addison-Wesley, Reading, MA, 1958).
[36] M. R. C. MacDowell and J. P. Coleman, *Introduction of the Theory of Ion-Atom Collisions* (North-Holland, Amsterdam, 1970).
[37] D. S. F. Crothers, J. Phys. B **15**, 2061 (1982).
[38] N. C. Sil, Proc. Phys. Soc. London **75**, 194 (1960).
[39] D. S. F. Crothers, Comments At. Mol. Phys. **15**, 15 (1984).
[40] A. R. Edmonds, *Angular Momentum in Quantum Mechanics* (Princeton University, Princeton, NJ, 1957).
[41] *Tables of Integral Transforms,* edited by A. Erdelyi (McGraw-Hill, New York, 1954), Vol. 1.
[42] W. J. Thompson, *Computing in Applied Science* (Wiley, New York, 1984).
[43] W. Brandt and G. Lapicki, Phys. Rev. A **20**, 465 (1979).
[44] P. A. Amundsen, L. Kocbach, and J. M. Hansteen, J. Phys. B **9**, L203 (1976).
[45] B. Raith, S. Divoux, and B. Gonsior, Nucl. Instrum. Methods B **10/11**, 169 (1985).
[46] *Handbook of Mathematical Functions,* edited by M. Abramowitz and I. A. Stegun (National Bureau of Standards, Washington, D.C., 1965), p. 445, Eq. (10.2.35).
[47] G. Arfken, *Mathematical Methods for Physicists,* 3rd ed. (Academic, Orlando, 1985), p. 428.
[48] J. F. Reading, A. L. Ford, J. S. Smith, and R. L. Becker, IEEE Trans. Nucl. Sci. **NS-30**, 1079 (1983).
[49] J. Macek and S. Alston, Phys. Rev. A **26**, 250 (1982).
[50] M. Rodbro, E. Horsdal-Pedersen, C. L. Cocke, and J. R. MacDonald, Phys. Rev. A **19**, 1936 (1979).
[51] D. J. Land, M. D. Brown, D. G. Simons, and J. G. Brennan, Nucl. Instrum. Methods **192**, 53 (1982).
[52] D. J. Land, D. G. Simons, and M. D. Brown, Nucl. Instrum. Methods **214**, 35 (1983); D. J. Land and D. G. Simons, Nucl. Instrum. Methods B **4**, 239 (1984).
[53] J. Theis and B. Müller, Phys. Rev. A **24**, 89 (1981).
[54] K. A. Ter-Martirosyan, Zh. Eksp. Teor. Fiz. **22**, 284 (1952).